High-gradient millimeter-wave accelerator on a planar dielectric substrate*

Marc E. Hill, Chris Adolphsen, W. Baumgartner, Richard S. Callin, Xintian E. Lin, Mike Seidel, Tim Slaton, and David H. Whittum

Stanford Linear Accelerator Center, Stanford University, Stanford, CA 94309

Abstract

We report the first high gradient studies of a millimeter-wave accelerator, employing for the first time a planar dielectric accelerator, powered by means of a 0.5-A, 300-MeV, 11.424-GHz drive electron beam, synchronous at the 8-th harmonic, 91.392 GHz. Embedded in a ring-resonator circuit within the electron beamline vacuum, this structure was operated at 20 MeV/m, with a circulating power of 200 kW, for 2×10^5 pulses, with no sign of breakdown, dielectric charging or other deleterious high-gradient phenomena. We also present the first measurement of the quadrupolar content of an accelerating mode.

Submitted to Physics Review Letters

High-gradient millimeter-wave accelerator on a planar dielectric substrate

Marc E. Hill[†]

Department of Physics, Harvard University, Cambridge, MA 02138

Chris Adolphsen, W. Baumgartner, Richard S. Callin, Xintian E. Lin, Mike Seidel, Tim Slaton, and David H. Whittum

Stanford Linear Accelerator Center, Stanford University, Stanford, CA 94309

(Dated: October 26, 2000)

We report the first high gradient studies of a millimeter-wave accelerator, employing for the first time a planar dielectric accelerator, powered by means of a 0.5-A, 300-MeV, 11.424-GHz drive electron beam, synchronous at the 8-th harmonic, 91.392 GHz. Embedded in a ring-resonator circuit within the electron beamline vacuum, this structure was operated at 20 MeV/m, with a circulating power of 200 kW, for 2×10^5 pulses, with no sign of breakdown, dielectric charging or other deleterious high-gradient phenomena. We also present the first measurement of the quadrupolar content of an accelerating mode.

High energy physics requires accelerators operating at extreme gradients, in excess of 100 MV/m, and this requires high-frequency electromagnetic waves, to avoid trapping of itinerant beamline particles, and to avoid machine self-destruction by single-pulse ohmic heating and the resulting cyclic stress [1]. The conception and development of such a high gradient collider has proved elusive in recent decades, yet continues to attract broad interest. Several generations of physicists have devoted themselves to elaborations on Hansen's concept of the resonant cavity [2], and the use of disk loaded structures. Unfortunately these fail at high-fields [3], and are difficult to fabricate at short wavelengths [4]. Meanwhile, a workable accelerator structure concept is in itself only half the solution, for a power source is required, and these have taken five decades to develop at lower frequencies [5]. In this Letter we report experimental studies of a possible solution to both problems, in the form of a new concept, a planar dielectric accelerator, built and tested at high gradient in a "two-beam accelerator" configuration.

The principle of the linear electron accelerator is *synchronism*, the matching of the phase velocity of the wave to the near speed of light electron beam. This insures that a particle traversing the structure witnesses a *non-zero* accelerating gradient. Beyond this, one is interested to achieve a *high* accelerating gradient for a given input power—a high "shunt impedance"— and in a conventional structure this is accomplished by loading smooth circular pipe with periodically spaced annuli that shape the field [6]. These "disks" pose serious fabrication problems at short wavelengths, not so much in their feature size and μm -scale tolerances, as in the problem of bond-
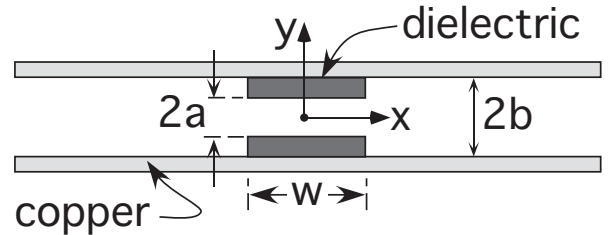
FIG. 1: A cross-section of the planar dielectric accelerator. The particle beam travels in the z direction, out of the page, with orbit centered on the origin. The electromagnetic properties of the accelerator are determined by the relative permittivity ε_r of the dielectric, the copper gap b, and the dielectric gap a and width w.

ing copper at the current-carrying ("rf") joints [4].

A completely different approach is the planar dielectric accelerator (PDA) seen in Fig. 1. Here synchronism is achieved by means of a dielectric liner with cross-section *uniform* in the beam direction z, much as in the related concept of the cylindrical dielectric guide proposed and studied at centimeter-wavelengths [7]. At millimeter wavelengths a cylindrical geometry is difficult to fabricate, and this motivates the planar design. In this geometry, the power required to establish an accelerating gradient, G, is $P \sim G^2 w(b-a)/Z_0$ and the corresponding shunt impedance per unit length is $r = G^2/2\alpha P$, where α is the field attenuation parameter in the structure, determined by the loss-tangent of the dielectric, resistive loss in the copper, and the group velocity ratio $v_g/c \approx 1/\varepsilon_r$, with c the speed of light [8]. The implication of these scalings is that high-shunt impedance may be achieved in a low-loss dielectric. For the proof-of-principle work reported here, we concentrate on alumina

ceramic, with relative permittivity $\varepsilon_r = 9.5$, and loss-tangent $\tan\delta \approx 10^{-3}$. Meanwhile high thermal conductivity and dielectric strength may ultimately favor the use of diamond [8].

Analysis of the geometry of Fig. 1 reveals several additional advantages of the design. Of specific interest for high-gradient operation, the field at the conducting surface $(y = \pm b)$ is given by $E_y/G \approx 1/\sqrt{\varepsilon_r - 1}$, while the field at the dielectric surface $(y = \pm a)$ is a factor of two or so larger, depending on the ratio b/a. This result, that the surface field to accelerating field ratio E_y/G is less than 1, stands in contrast to a ratio of 2 typical in conventional disk-loaded structures. As this figure appears in the exponent of the Fowler-Nordheim relation, the consequences are promising for field-emission, and associated phenomena such as breakdown [9]. Other advantages of this open-sided structure are good vacuum conductance, wide beam aperture, and heavy wakefield damping.

For purposes of a collider, the geometry of Fig. 1 is consonant with mm-wave drive, e.g., a "klystrino" [10], or beam drive as in the "two-beam accelerator"[11]. In fact, to test the structure at high-fields, given the absence of a high-power mm-wave source, it is most natural to employ a relativistic electron beam to drive the structure. In such a "relativistic klystron", we may employ a beam of intra-pulse current I_0, bunched at angular frequency ω_0 to drive a structure at the n-th beam harmonic, $n\omega_0$, producing a gradient $G_b = rI_b(1 - e^{-\alpha L})$ where L is the structure length, and $I_b = I_0 e^{-n^2\omega_0^2\sigma_t^2/2}$ is the n-th current harmonic, with σ_t the rms length of each micro-bunch. A still-higher gradient can be achieved by coupling power from the structure output, to the input. With such "recirculation", the gradient at the structure exit is the real part of

$$G_r = rI_b(1 - e^{-\tau})/(1 - he^{-\tau}) \qquad (1)$$

where $h = Ae^{i\phi}$ describes the attenuation, A, and phase, ϕ, of the recirculation arm. The maximum power generated is then $P = |G_r|^2/2\alpha r$.

To prove these principles of operation we selected as our beam driver a 300 MeV linac providing a 100-ns, 0.5-A beam at 10 Hz, bunched at 11.424 GHz [3]. We chose the $n = 8$ harmonic corresponding to a 91.392 GHz structure, and after some intervening steps, arrived at the experimental layout depicted in Fig. 2. This schematic illustrates an rf detector circuit situated outside the beamline vacuum, receiving a mm-wave signal from an accelerator circuit inside the beamline vacuum envelope. The circuit consists of a planar dielectric accelerator, with input connected to output by means of a slotted waveguide U-bend functioning as a squeeze-type phase-shifter. Circulating power is monitored by means of a single-hole coupler mounted on the U-bend, and this monitor signal passes through a vacuum window to the receiver. We describe each of these components of the accelerator circuit in turn, followed by details of high-power studies with the circuit as a whole.
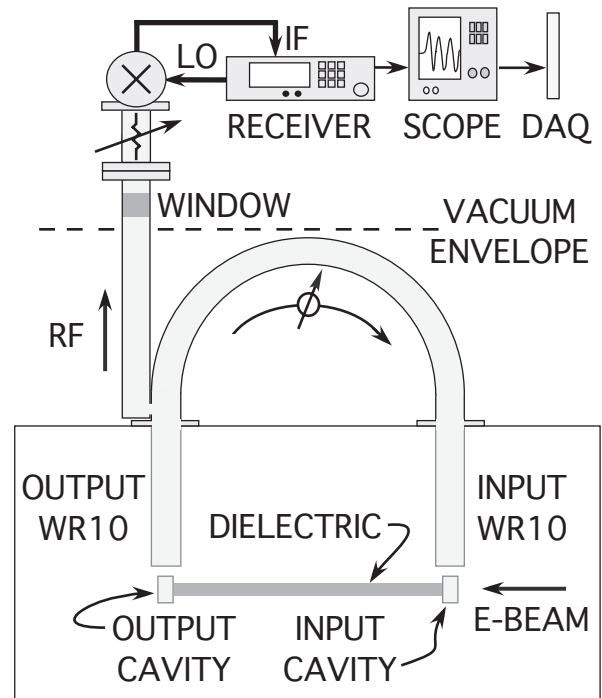

FIG. 2: Layout for high-power tests of the miniature dielectric accelerator, depicting the synchronous drive beam, a recirculation arm consisting of a squeeze-type phase shifter fashioned from a WR10-waveguide U-Bend, a single-hole WR10 output coupler, followed by a vacuum window, a variable attenuator and a heterodyne receiver mixing the 91.4-GHz (RF) signal down to a 300 MHz intermediate frequency (IF) waveform that is sampled by a 5-GS/s scope and passed to the data acquisition system (DAQ) for off-line analysis.

The window consists of WR10 oxygen-free electronic-grade (OFE) copper waveguide, operated in fundamental TE_{10}-mode, with a brazed-in slab of Wesgo AL-995 alumina ceramic dielectric functioning as a standing-wave "1-λ" window, with design dimensions determined by analytic scalings. Prior to incorporation in the accelerator circuit the completed window-assembly was subjected to vector network analyzer (VNA) measurements with transmission and reflection coefficients S_{12} and S_{11} consistent with a relative permittivity $\varepsilon_r \approx 9.48\pm.03$ [12], and agreeing well with numerical simulation via the finite-difference code $GdfidL$ [13]. The window provides voltage standing wave ratio (VSWR) less than 1.1, with insertion loss of 0.5 dB at 91.392 GHz.

The squeeze-type phase-shifter consists of a 180° WR10 E-Bend formed from extruded OFE copper, with a slot on the broad wall formed by wire electro-discharge machining (EDM). The slot permits a change in the phase length of the guide by adjustment of the slot width, i.e., "squeezing", accomplished via a 10×-motion reduction lever and vacuum feedthrough providing linear motion steps of 25 μm and yielding 2.5 μm steps in guide

width. Bench-measurements for phase-shift versus actuator setting agree well with an analytic result for phase-shift versus wall displacement and show that the full 360° range can be reached with 250 μm of width-adjustment and good linearity [15]. The insertion loss for the phase-shifter was 0.9 dB. A 50-dB single-hole coupler integrated into the phase-shifter on the output arm of the structure allowed for monitoring of the recirculation power level.

The dielectric accelerator circuit itself consists of $0.3\times0.8\times25.4$ mm^3 alumina ceramic strips brazed onto copper substrates with input and output waveguide and coupler cells machined using stub EDM. To achieve synchronism and coupling-cavity tune in this structure, iteration on the bench was necessary, between EDM fine tuning of the cavities, screw adjustment of the substrate separation, and VNA measurements employing a non-resonant bead pull [14]. After three iterations bead-pull data indicated that the tuning procedure had converged, with the phase velocity matching c within 0.1%. Meanwhile, the decay length, $1/\alpha \approx 73$ mm, consistent with a dielectric loss tangent of 10^{-3}, and copper loss typical of our chemically cleaned OFE copper WR10, about 30% higher than ideal[8]. The result was a matched 2-port accelerator circuit.

With dimensions $w \approx 800\mu$m, $a \approx 360\mu$m, and $b \approx 660\mu$m, the theoretical pencil-beam shunt impedance for our design is a high $r \approx 63$ MΩ/m. In practice, due to the finite size of the probe beam, and the dependence of the accelerating field on transverse coordinates x and y, the effective shunt-impedance is lowered. This field dependence is determined from simulation with *GdfidL*, while the beam profile at the structure is inferred from profile screen measurements located at a structure image. The structure itself is located at the focus of a quadrupole triplet that provides a 200μm$\times300\mu$m Gaussian beam profile, for which we calculate an effective figure of 50 MΩ/m.

Microwave detection in the circuit of Fig. 2 was accomplished with a heterodyne receiver circuit consisting of a Hewlett-Packard HP11970W 18×-harmonic mixer, and an HP 8563 spectrum analyzer functioning as a signal generator, and a tuned receiver, providing a tunable rf local oscillator signal at 5 GHz, and receiving a 300-MHz fixed-tuned IF. The IF is read by a Tektronix 684B 5-GS/s digitizing real-time oscilloscope with 1-GHz input bandwidth and stored to disk for off-line analysis, together with a fast toroid waveform for the same pulse. From the 300-MHz IF pulse, the amplitude V_{IF} and phase ϕ are extracted by digitally mixing the IF waveform down to baseband, and applying a Butterworth filter. This procedure was calibrated by means of a continuous-wave 91.4 GHz signal generator of adjustable amplitude, with power levels measured via an HP-W8486 power-meter. A sample IF envelope is shown in Fig. 3, together with the corresponding toroid waveform. Also shown is the mm-wave phase, from which one can see that the bunch phase is maintained within 5° of X-band or 40° at 91.4 GHz.
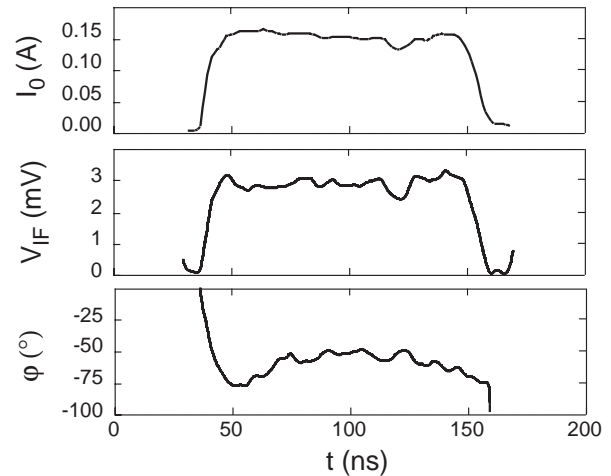
With this apparatus, three mm-wave power studies

FIG. 3: Illustrating the beam-current waveform, the envelope of the 300-MHz IF voltage waveform, and the IF phase.

were performed: a low-power, high-gradient test of a single resonant cavity, a low-power test of the PDA without recirculation, and a high-power test of the PDA in the traveling-wave resonator configuration.

The first test employed a single resonant cavity with WR10 output and a vacuum window and confirmed: feasibility of beam delivery through a 680 μm diameter beam tube, without damage to the structure, the operability of the window at high-field, and operation of the mm-wave receiver with the relatively simple equivalent circuit of the single cavity. Moreover, this study permitted a direct check of the $n = 8$ harmonic component, I_b. The expected output power in this configuration is

$$P_c = \frac{1}{4}\left[\frac{R}{Q}\right]\frac{Q_L^2}{Q_e}I_b^2\cos^2\psi, \qquad (2)$$

where the tuning angle, $\tan\psi = Q_L(\omega_r/\omega - \omega/\omega_r)$, with ω_r the cavity resonance angular frequency, and $\omega = n\omega_0$ the drive angular frequency. The loaded quality factor, Q_L, external quality factor, Q_e, and ω_r are determined by VNA bench measurements on the resonator. The beam coupling parameter, $[R/Q]$ is calculated using *GdfidL* [16]. The result is compared with high-power data in Fig. 4, giving good agreement for the expected bunch length of $\sigma_t = 1.2$ ps, corresponding to $I_b/I_0 = 0.8$. This test produced a peak power of 1 kW, corresponding to a 15 MV/m gradient, and 0.8 MV/m field at the window.

The second test employed the dielectric accelerator circuit of Fig. 2, but with the recirculation and coupler arm removed. In their place, the input and the output waveguide were each connected to 2" lengths of stainless steel WR10 slotted on the narrow wall and functioning as matched 5 dB attenuators. These were followed by rf windows, permitting detection and analysis of beam-induced signals seen from the input, and the output guide. This test confirmed transmission of the beam
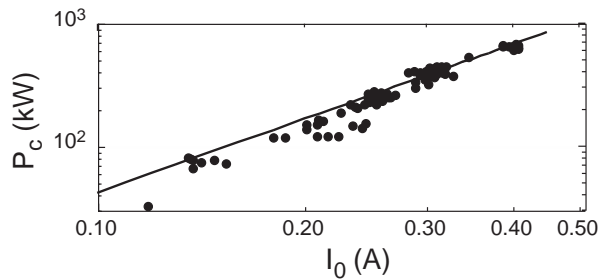
FIG. 4: Power output from a 91.4 GHz cavity resonator driven by an X-band bunched beam overlayed with the expected power result of Eq. (2).
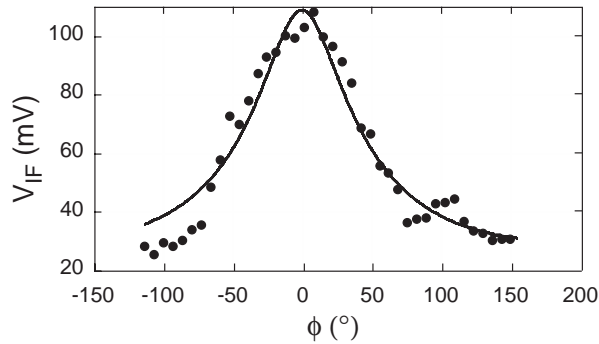

FIG. 5: Peak RF voltage output of the circuit in Fig. 2 versus recirculator phase shift, overlayed with the theoretical result of Eq. 1.

through the 720 μm slit of the 2.54 cm long structure, and produced 24 kW in the structure with a drive current of $I_0 \approx 0.5$ A. The rf window handled 4 kW corresponding to a field in the waveguide of 1.6 MV/m. From the figures for power, current, and bunch-length, one may infer a shunt-impedance per unit length of $r \approx 42$ MΩ/m and beam-induced gradient $G \approx 7$ MV/m at the structure output. This figure for shunt impedance is within 16% of the theoretical value, after convolution with the beam profile.

Finally, with all components checked out separately, we tested the circuit of Fig. 2, including the recirculation arm. The effect of the phase-shifter on recirculation is seen in Fig. 5 overlaid with the result of Eq. (1), fit with the attenuation parameter A, corresponding to 2 dB. This figure for A is consistent with the insertion loss of the phase shifter (0.9 dB) together with the attenuation through the input and output waveguide (0.5 dB each).

In addition, in this setup it was possible to scan the beam across the structure, and in this way map the transverse dependence of the shunt-impedance, permitting inference of the accelerating mode quadrupole component. The result is seen in Fig. 6. Overlaid is the theoretical result incorporating the convolution of the beam profile with the transverse field dependence determined from *GdfidL*, and scaled from 50 MΩ/m to 42 MΩ/m to fit the
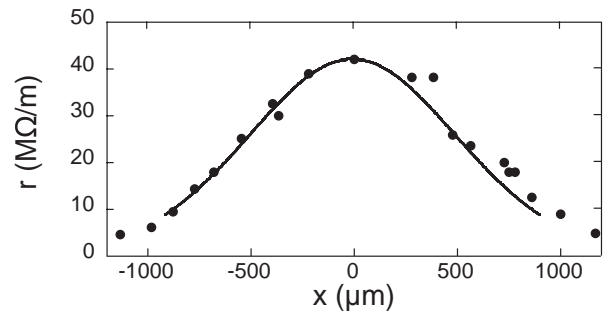

FIG. 6: Effective shunt impedance versus beam position, overlayed with the theoretical result scaled down by 16% to fit the peak. The x coordinate is as in Fig. 1, with origin shifted to fit the peak.

peak.

In these studies the PDA circuit handled a circulating power of 200 kW reliably for $\sim 2 \times 10^5$ pulses (about two weeks), corresponding to an accelerating gradient of 20 MV/m. Experience at lower frequencies indicates that at these field levels one may be concerned with breakdown[9]. Ceramic charging from beam scraping is also a concern in principle. We saw no sign of either of these phenomena. We have yet to find a physics obstacle to extension to higher gradients.

REFERENCES

[1] D.H. Whittum, in *Advanced Accelerator Concepts*, W. Lawson, C. Bellamy and D.F. Brosius, eds., AIP Conf. Proc. **472** (AIP, New York, 1999) pp. 72-85.

[2] W. W. Hansen, *J. Appl. Phys.* **9** (1938) pp. 654-663

[3] C. Adolphsen *et al.*, in *Proceedings of the 20th International Linac Conference (Linac 2000)*, Monterey, California, 21-25 Aug 2000, SLAC-PUB-8573, *to be published.*

[4] P.J. Chou, *et al.*, *Advanced Accelerator Concepts*, AIP Conf. Proc. **398** (AIP, New York, 1997) pp. 501-517.

[5] G. Caryotakis, *IEEE Trans. Plasma Sci.* **22**, pp. 683-691, 1994.

[6] D. Whittum, in *Techniques and Concepts of High-Energy Physics*, T. Ferbel, ed., (Kluwer, Amsterdam, 1999) Vol. X, pp. 387-486.

[7] P. Zou, *et al.*, *Proceedings of the 1999 Particle Accelerator Conference* (IEEE, New York, 1999) pp. 3618-3620

[8] M.E. Hill, *et al.*,"Planar Dielectric Accelerator

Structures at W-Band", submitted to *Rev. Sci. Instrum.*, SLAC-PUB-8666.

[9] J.W. Wang and G.A. Loew, in *Frontiers of Accelerator Technology*, S.I. Kurokawa, M. Month and S. Turner, eds., (World Scientific, Singapore, 1999) pp. 768-794.

[10] G. Caryotakis, *et al.*, in *Proceedings of the SPIE International Symposium on Optical Science, Engineering and Instrumentation*, (SPIE, San Diego, 1997) pp. 3114-3120.

[11] G. Westenskow *et al.*, in *Proceedings of the 1995 Particle Accelerator Conference* (IEEE, New York, 1996)

pp. 737-739

[12] M.E. Hill, *et al.*,"High-Power Vacuum Window in WR10", *IEEE Trans. MTT* (to be published).

[13] W. Bruns, *IEEE Trans. Magn.* **32** (1996) pp.1453-1456.

[14] C.W. Steele, *IEEE Trans. MTT* **14** (1966) pp. 70-74

[15] M.E. Hill, *et al.*,"High-Power Squeeze-Type Phase-Shifter at W-Band", submitted to IEEE Trans. MTT.

[16] M.E. Hill, *et al.*,"Beam-Cavity Interaction Circuit at W-Band", *IEEE Trans. MTT* (to be published).